Research Square

Preprints are preliminary reports that have not undergone peer review.
They should not be considered conclusive, used to inform clinical practice,
or referenced by the media as validated information.

Real-Time and Real-World Gait Monitoring on a Wearable Device: A Fully Embedded System for Parkinson's Disease

Jelina Unger
Friedrich-Alexander-Universität Erlangen-Nürnberg
Goran Madzar
Medtech Ingenieur GmbH
Syrine Slim
Friedrich-Alexander-Universität Erlangen-Nürnberg
Ann-Kristin Seifer
Friedrich-Alexander-Universität Erlangen-Nürnberg
Iliya Ghotbiravandi
Friedrich-Alexander-Universität Erlangen-Nürnberg
Majid Dareini
Friedrich-Alexander-Universität Erlangen-Nürnberg
Franz Marxreiter
Universitätsklinikum Erlangen
Juergen Winkler
Universitätsklinikum Erlangen
Heiko Gassner
Universitätsklinikum Erlangen
Bjoern M. Eskofier
Ludwig-Maximilians-Universität München
Hamid Moradi
hamid.moradi@fau.de

Universitätsklinikum Erlangen

Method Article

Keywords: IMU, Gait analysis, Real-time, Parkinson's Disease, Home monitoring, On-device

Posted Date: September 11th, 2026

DOI: https://doi.org/10.21203/rs.3.rs-10711436/v1

License: This work is licensed under a Creative Commons Attribution 4.0 International License.
Read Full License

Additional Declarations: Competing interest reported. At the time the study was conducted, Jelina Unger was a student at Friedrich-Alexander-Universität Erlangen-Nürnberg (FAU) and was employed as a working student by Medtech Ingenieur GmbH. Goran Madzar is the managing director at Medtech Ingenieur GmbH. Medtech Ingenieur GmbH manufactured the sensor system used in this study.

Real-Time and Real-World Gait Monitoring on a Wearable Device: A Fully Embedded System for Parkinson's Disease

Jelina Unger[1,2], Goran Madzar[2], Syrine Slim[1], Ann-Kristin Seifer[1], Iliya Ghotbiravandi[1], Majid Dareini[1], Franz Marxreiter[3,4], Juergen Winkler[3], Heiko Gassner[3,5], Bjoern M. Eskofier[1,6], Hamid Moradi[1,3*]

[1]Department Artificial Intelligence in Biomedical Engineering, Friedrich-Alexander-Universität Erlangen-Nürnberg, Erlangen, Germany.
[2]Medtech Ingenieur GmbH, Erlangen, Germany.
[3]Department of Molecular Neurology, University Hospital Erlangen, Erlangen, Germany.
[4]Center for Movement Disorders, Passauer Wolf, Bad Gögging, Neustadt an der Donau, Germany.
[5]Fraunhofer Institute for Integrated Circuits IIS, Erlangen, Germany.
[6]Chair of AI-Supported Therapy Decisions, Ludwig-Maximilians-Universität München, Munich, Germany.

*Corresponding author(s). E-mail(s): hamid.moradi@fau.de;
Contributing authors: jelina.unger@murena.io; madzar@medtech-ingenieur.de; syrine.slim@fau.de; ann-kristin.seifer@fau.de; iliya.ghotbiravandi@fau.de; majid.dareini@fau.de; Franz.Marxreiter@passauerwolf.de; juergen.winkler@uk-erlangen.de; heiko.gassner@uk-erlangen.de; eskofier@lmu.de;

Abstract

Background: Real-time gait analysis is essential for capturing transient gait alterations as they occur, enabling assessment of mobility beyond delayed retrospective analysis. This capability is particularly relevant in Parkinson's disease (PD), where gait characteristics fluctuate throughout daily activities and may

benefit from continuous monitoring. However, many existing gait analysis systems rely on offline processing or laboratory-based equipment, limiting their applicability for long-term real-world monitoring. This study aims to develop and validate a wearable, foot-worn sensor system that enables real-time, on-device gait analysis suitable for long-term monitoring of activities of daily living in patients with PD.

Methods: We developed a two-stage algorithm consisting of motion detection followed by gait event detection. Algorithm parameters were optimized using four-fold cross-validation on home recordings of 28 individuals with PD (FallRiskPD), replayed as a simulated real-time data stream. The finalized system was subsequently validated under true real-time conditions on an independent dataset of 18 healthy participants (TestES), performing supervised instructed and self-directed walking tasks, validating end-to-end system operation including wireless data transmission and real-time gait parameter delivery.

Results: The hardware achieved an F1-score of 85.4% for stride segmentation on home recordings from patients with PD. Relative to a state-of-the-art offline reference method, temporal gait parameters had an absolute percentage error of 0.3% for stride time, 6.5% for swing time, and 3.6% for stance time. Under true real-time evaluation of the complete end-to-end system, the implementation achieved an average runtime of 1.245 ± 0.578 ms per update, with a mean parameter-delivery delay of 1.169 ± 0.525 s using 3-second analysis windows, demonstrating continuous real-time operation.

Conclusions: This work presents a portable real-time gait analysis system with fully embedded processing for wearable deployment. By enabling low-latency, on-device computation of temporal gait parameters, the proposed solution supports continuous mobility assessment in daily-life settings and provides a foundation for future real-time feedback and intervention strategies in PD.

Keywords: IMU, Gait analysis, Real-time, Parkinson's Disease, Home monitoring, On-device

1 Background

Gait provides a sensitive and objective marker of functional status and change over time, with strong associations to established measures of functional mobility [1, 2]. In neurodegenerative disorders such as Parkinson's Disease (PD), gait impairment is one of the key manifestations of motor dysfunction, characterized by progressive deterioration and transient gait disturbances, including daily fluctuations, freezing of gait, and falls, which substantially compromise mobility and independence. Furthermore, sudden motor deficits are often difficult to capture using conventional clinical assessments [3]. Consequently, quantitative gait assessment plays a central role in detecting changes in gait performance, evaluating treatment effects, and enabling timely interventions during daily life [4–7].

Wearable gait analysis systems and particularly shoe-mounted Inertial Measurement Unit (IMU)s enable objective capture of spatio-temporal gait parameters in

real-world environments [8–11]. To quantify clinically relevant aspects of gait impairment, a broad range of computational approaches has been developed to estimate macro-level mobility measures, such as daily activity patterns and risk of falls, as well as micro-level gait characteristics, including stride segmentation, gait event detection, and spatio-temporal stride parameters [10–13]. Machine learning and deep learning approaches have gained substantial traction for these tasks, particularly for offline gait analysis, due to their ability to capture complex and non-linear patterns in wearable sensor data [4, 14–17].

While macro-level analysis is able to tolerate offline processing and substantial latency, micro-level gait parameters at the stride and event level impose stringent real-time and low-latency requirements, substantially increasing computational demands and system complexity [10, 18]. Although several studies have demonstrated the feasibility of real-time gait event detection using data-driven approaches, lightweight implementations suitable for continuous wearable deployment remain limited [19, 20]. For example, recurrent neural networks have been applied for gait event detection under clinical conditions [21], while hybrid approaches combining machine learning classifiers with temporal models have achieved low-latency detection using multi-sensor configurations and external processing units [20, 22]. However, their reliance on powerful processing units, multi-sensor configurations, distributed system architectures, or predefined tasks, which can increase computational burden, processing time, and energy demand, limiting their applicability for continuous, unobtrusive gait monitoring in daily-life settings[23, 24].

In contrast to data-driven approaches, rule-based algorithms have been widely adopted for real-time analysis of micro-level gait parameters due to their ability to directly exploit biomechanical characteristics of inertial signals, such as characteristic peaks, zero-crossings, and physiologically constrained temporal relationships [25–29]. These models enable deterministic, low-latency, and fully on-device execution without reliance on training data or computationally intensive inference [26–29]. Their deterministic behavior and low computational complexity enable efficient on-device execution, which has facilitated successful deployment on embedded wearable platforms [20, 27, 29, 30], making them particularly well suited for continuous stride-level monitoring during activities of daily living.

Despite their suitability for low-latency, on-device execution, rule-based gait analysis pipelines face challenges during continuous real-time operation due to the limited computational and energy resources of wearable systems, particularly in daily-life conditions [20, 30, 31]. Prior work has highlighted a fundamental trade-off between sampling resolution and battery lifetime, where reducing the sampling frequency can extend operational duration but may attenuate high-frequency signal components critical for detecting subtle gait events and abnormalities [20]. To address this challenge, motion-aware frameworks have been explored in which activity recognition selectively activates sensing or processing, reducing unnecessary computation during periods without gait activity [30, 31]. Such strategies provide a pathway toward energy-efficient continuous gait monitoring on wearable platforms.

Beyond computational constraints, the clinical and real-world validation of real-time embedded gait analysis systems remains limited. Many systems are primarily

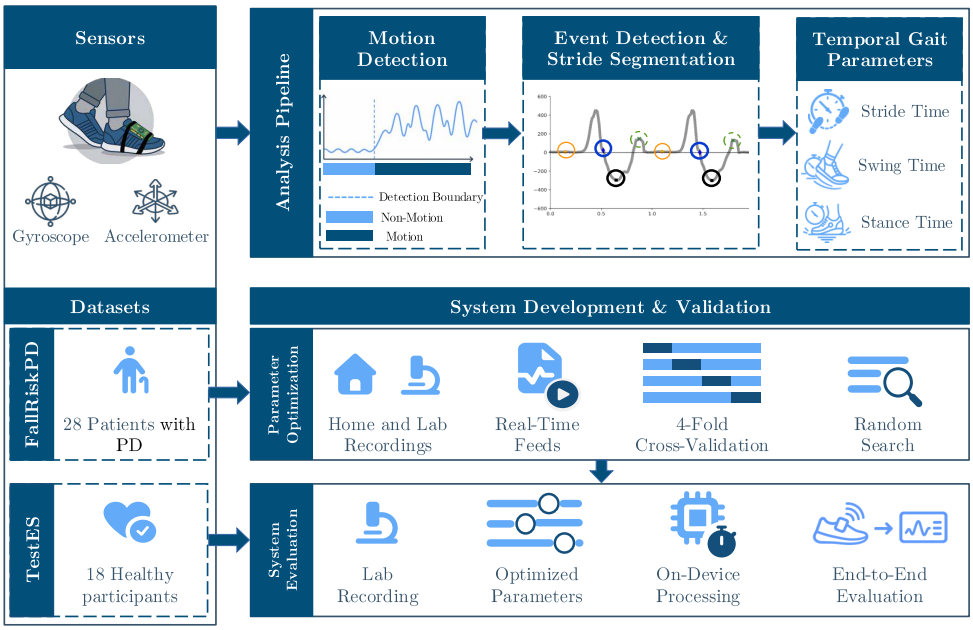


Fig. 1: Overview of the development and evaluation framework for real-time, on-device gait analysis. Parameters were optimized using laboratory and home recordings processed under simulated real-time conditions, with random search and four-fold cross-validation. The optimized configuration was subsequently deployed on the wearable device and evaluated as an end-to-end pipeline using laboratory recordings.

evaluated in healthy participants under controlled laboratory conditions [13, 20, 28, 29]. However, gait characteristics and motor impairments in clinical populations may influence detection performance and timing accuracy [32], highlighting the importance of evaluating algorithms using data from individuals with PD [10]. Furthermore, true real-world mobility introduces additional variability through unsupervised activities of daily living, irregular movement patterns, and context-dependent gait adaptations that are often not captured during supervised recordings [12]. Therefore, a real-time, fully embedded gait analysis system validated in individuals with PD and under real-world mobility conditions remains needed.

This study aims to design, implement, and validate a lightweight wearable real-time gait analysis system for the continuous gait assessment of activities of daily living in individuals with PD. The proposed system performs all processing on-device using shoe-mounted IMU sensors to deliver temporal gait parameters in real time during walking bouts while operating under strict embedded constraints on runtime and latency. The system was optimized and evaluated using unsupervised, real-world recordings from individuals with PD, demonstrating accurate and resource-efficient gait analysis beyond controlled laboratory settings, and subsequently validated for live, end-to-end real-time performance on an independent cohort of healthy participants.

Figure 1 provides an overview of our approach, which is detailed in the following section.

2 Methods

2.1 Datasets

Two datasets were used in this study, each serving a distinct methodological purpose. The FallRiskPD dataset consists of long-term home recordings from patients with PD and was used for algorithm development, parameter tuning, and evaluation under real-world conditions using a cross-validation (CV) strategy. These recordings were converted into real-time feeds using a real-time simulation framework, allowing realistic execution and optimization of the algorithms. To assess the performance of the complete end-to-end system under true real-time conditions, we collected an independent dataset called TestES. The TestES dataset was collected using the final hardware and software configuration, exclusively to evaluate the finalized system operating in real-time.

2.1.1 FallRiskPD

This dataset comprises recordings from 28 individuals with PD, including supervised in-laboratory gait assessments and a single day of unsupervised home monitoring (Table 1). During laboratory visits, participants completed standardized gait assessments under supervision, including four 10-m walk tests at preferred, fast, and slow speeds, a 2-min walk test, and the Timed-Up-and-Go test. Home recordings were acquired during unsupervised activities of daily living using the same wearable sensors.

In this dataset, the sensor specifications comparable to the final real-time system in terms of sampling rate, measurement range, and sensor placement, ensuring ecological validity. Although the data were originally recorded offline, they were fed to the processing pipeline as a simulated real-time stream, allowing the online gait event detection and stride characterization algorithms to be validated under conditions representative of deployment. All data were recorded using IMUs equipped with tri-axial accelerometers (range $\pm 16\,\mathrm{g}$) and gyroscopes (range $\pm 1000\,^\circ/\mathrm{s}$) with the sampling rate of 102.4 Hz, attached to the instep of the shoes [12]. The study was approved by the local ethics committee of the Friedrich-Alexander-Universität Erlangen-Nürnberg, Germany (Re-No. 165_18B). All participants provided written informed consent prior to data collection.

2.1.2 TestES

This dataset comprises 18 healthy participants without physical impairment (Table 1).

The final system (an embedded device incorporating an IMU; specifications in subsection 2.2) was attached unilaterally to the instep of a shoe similar to the positioning of the FallRiskPD dataset, with nine participants wearing it on the left foot and nine on the right. Participants performed standardized walking tests, including eight 10-meter walks performed at three self-selected speeds (normal/preferred, fast, and slow), with 30 seconds of seated rest between speed conditions. Additionally, a five-minute

free-activity recording was acquired, during which participants could choose any walking pattern, standing, or sitting, to better emulate real-world behavior. During the initial 30 s of the five-minute recording, participants were instructed to walk and then stop to stand for 10 s. Finally, at the end of the recording session, the sensors were removed and placed on a table for 20 s before terminating the measurement.

This study was approved by the local ethics committee of the Friedrich-Alexander-Universität Erlangen-Nürnberg, Germany (Re-No. 106_13B). Prior to data collection, all participants were informed about the study procedure and data usage, and provided written informed consent.

Table 1: Participants' characteristics in the FallRiskPD and TestES dataset. Parameters are given as mean ± standard deviation or counts in the case of gender. UPDRS: Unified Parkinson's disease rating scale.

Demographics

Dataset	Sex (f/m)	Age [year]	Height [cm]	Weight [kg]	UPDRS III
FallRiskPD	(7/21)	63.7 ± 7.2	174.6 ± 8.8	77.1 ± 15.3	17.0 ± 8.1
TestES	(7/11)	30.6 ± 8.6	174.8 ± 10.2	73.2 ± 11.9	-

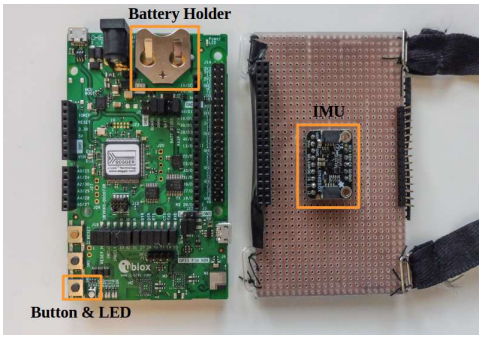
Gait Recordings

Dataset	Recordings [N]	Recording Time [min]	Recording / Subject [min]	Strides [N]	Strides / Subject [N]
FallRiskPD-Lab	28	751.0	26.8 ± 17.5	19789	706.7 ± 178.8
FallRiskPD-Home	28	15300.3	546.4 ± 98.8	157862	5050.6 ± 2935.8
TestES	18	229.8	12.7 ± 1.5	7813	434 ± 49

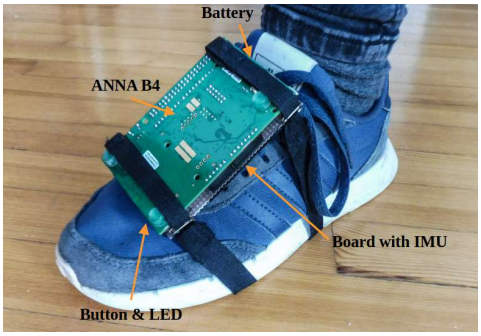
2.2 Embedded System Architecture

The embedded system comprises a microcontroller-based processing unit and an inertial measurement unit (IMU) for on-device gait parameter computation. To simplify development, the ANNA-B4 evaluation board was used as the processing platform, integrating a Nordic Semiconductor nRF52833 system-on-chip with an Arm Cortex-M4 processor including an FPU, operating at a 64 MHz system clock, with 512 kB internal flash memory and 128 kB RAM (Figure 2a and Figure 2b). The final system can be implemented using the ANNA-B4 chip, offering identical hardware specifications in a smaller form factor suitable for daily wearable use Figure 2d.

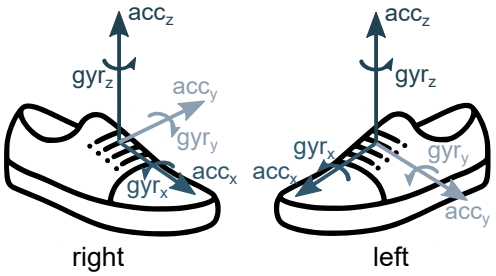
The data acquisition system comprises an LSM6DSO IMU (STMicroelectronics), which integrates a tri-axial accelerometer (range ±16 g) and a tri-axial gyroscope (range ±2000 °/s). The IMU operates in high-performance mode with a sampling rate of 100 Hz and a current consumption of 0.55 mA. Prior to data collection, the IMU was calibrated using the Ferraris method [33], implemented via the IMUCAL Python



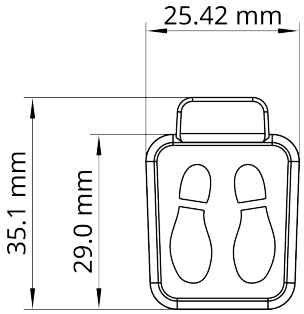
(a) Standalone system, showing the integrated push button for measurement control, the status LED (idle, connected, measuring, and error), and the onboard battery.



(b) System mounted on the foot, illustrating the placement of the embedded system on the shoe with the IMU positioned close to the foot.



(c) Coordinate systems used for IMUs of the left and right foot. *Gyr* stands for the gyroscope and *acc* for the accelerometer.



(d) Technical drawing of the final real-time system using the ANNA-B4 chip.

Fig. 2: Overview of the wearable embedded system: (a) hardware components; (b) sensor placement; (c) sensor orientation and coordinate system; and (d) dimensions of the final product.

package [34]. The data are captured in a sensor coordinate frame following the right-hand rule, where the x, y, and z correspond to the anteroposterior, mediolateral, and Superior-Inferior directions, respectively (Figure 2c).

Calculated gait parameters are transmitted in real time via Bluetooth 5.1 to an external client device for monitoring and visualization. In this study, a notebook computer with an Intel Core i5 (4 cores / 8 threads, 2.4 GHz base) and 16 GB RAM was used as the client; however, the same data stream can be received by other devices such as smartphones or tablets.

2.3 Algorithms

The algorithm is composed of two main components: **(A)** motion detection; **(B)** event detection and stride segmentation. Figure 3 illustrates the pipeline of event detection and stride segmentation.

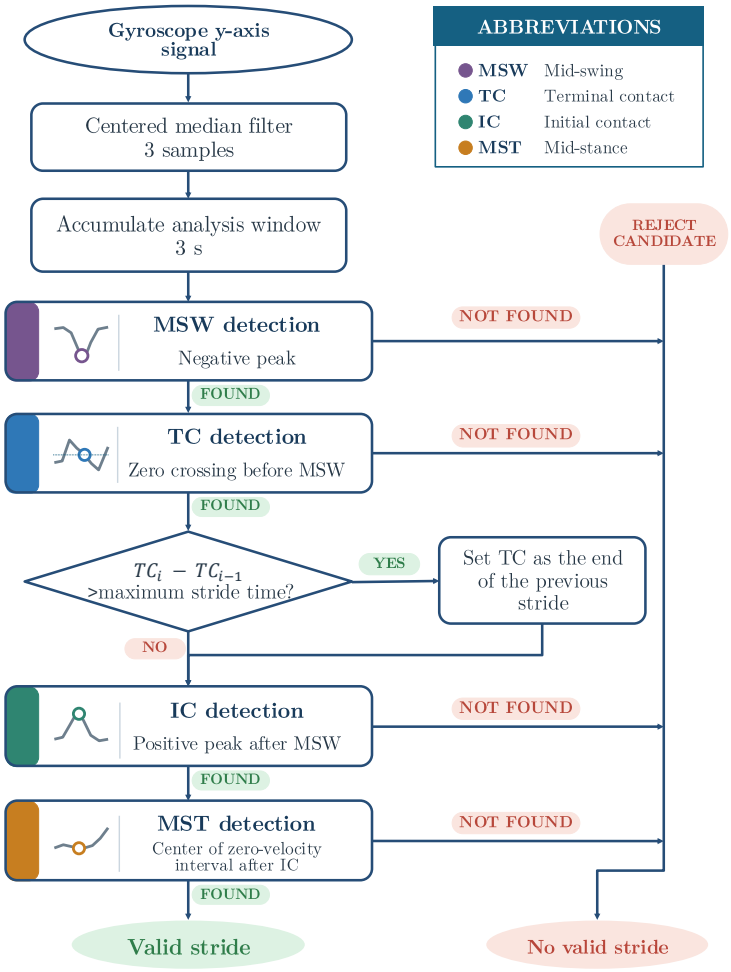


Fig. 3: Flowchart of the real-time stride-event detection algorithm. The Gyroscope (Gyr) y-axis signal is median-filtered and processed in 3-s analysis windows. Mid-swing (MSW), terminal contact (TC), initial contact (IC), and mid-stance (MST) are identified sequentially from characteristic signal features.

2.3.1 Motion Detection

Initially, the algorithm distinguishes between motion and non-motion states to identify activity and trigger the gait analysis pipeline. A threshold is applied to the absolute raw IMU signal to obtain sample-wise motion and non-motion labels. To ensure robust motion classification, preventing transient physiological pauses (e.g., the stance phase during walking) from being misclassified as non-motion, a validation window is appended to the end of each detected motion phase; all samples within this window remain labeled as motion. Subsequent steps of the pipeline are performed exclusively on data segments classified as motion. The selection of sensor modality (Accelerometer (Acc) or Gyroscope (Gyr)), threshold values, and validation window size was made using the FallRiskPD dataset (explained in subsection 2.5).

2.3.2 Event Detection and Stride Segmentation

Event detection and stride segmentation are integrated into a single algorithm applied to the Gyr-y signal. Each instance of event detection requires the fulfillment of specific conditions, which depend on various algorithm parameters. Figure 3 provides an overview of the complete processing pipeline. An example of the event detection delivery is shown in a supplementary video.

Analysis Window

For the gait analysis algorithm, sensor data are first buffered in a fixed-size overlapping window, sized to cover the longest possible stride plus the interval between terminal contact (TC) and mid-swing (MSW) of the following stride (a+d in Figure 4). This ensures accurate stride segmentation and boundary assignment with each window beginning at the previously detected MSW candidate. In the absence of detected strides, the maximum time from TC to MSW is maintained from the end of the previous window.

Mid-Swing

Initially, within each analysis window, all MSW events are detected as negative peaks in the gyroscope signal (black squares in Figure 4). A peak detection algorithm is implemented using a state-machine approach that identifies local minima based on characteristic changes in the signal slope.

Because gait speed affects the amplitude of the gyroscope signal, an adaptive threshold is used for MSW detection. The threshold is defined as 60 % of the average MSW amplitude over the preceding five strides. To ensure robustness against noise and irregular strides, the adaptive threshold is constrained within predefined lower and upper bounds, indicated by the dotted lines b and c in Figure 4. This approach allows the threshold to adapt to changes in gait speed while maintaining stable and reliable event detection. To reduce false-positive detection of MSW events caused by sharp transient peaks, the moving average over the preceding 8 samples is additionally required to remain below the adaptive threshold. This approach improves robustness while avoiding the processing delays associated with conventional signal filtering. A minimal stride-time constraint enforces a minimum temporal separation

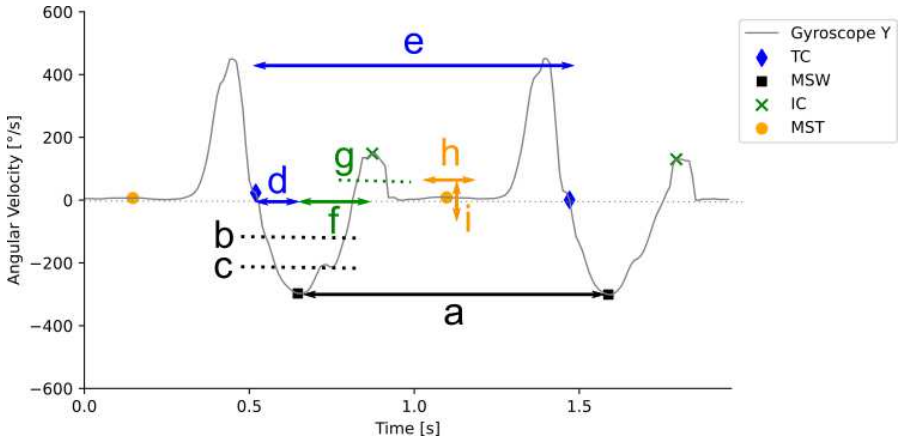


Fig. 4: Gyr y-signal of a section of gait with the marked events. For each event, the related algorithm parameters to find this event are visualized: (a) minimal stride time, (b) maximal and (c) minimal threshold for the amplitude of the MSW peak, (d) maximal distance between the TC and MSW, (e) maximal stride time, (f) maximum MSW-to-IC distance, (g) minimal amplitude of the initial contact (IC) peak, (h) minimal duration of the zero velocity window, and (i) amplitude margin of zero velocity.

between consecutive MSW events (arrow a in Figure 4). When multiple peak candidates occur within this interval, the peak with the highest absolute (i.e., most pronounced) amplitude is selected.

Terminal Contact

After an MSW event is detected, the preceding zero-crossing within a maximum permissible distance (arrow d in Figure 4) is identified as TC. Each TC marks the boundary between two consecutive strides: the start of the current stride and, if a preceding stride exists and the interval to its TC is shorter than the maximum stride time (arrow e in Figure 4), the end of that previous stride.

Initial Contact

The initial contact (IC) is defined as the positive peak occurring within a limited window following the MSW peak (arrow f in Figure 4), with an amplitude exceeding a predefined threshold (dotted line g in Figure 4).

Mid-Stance

The mid-stance (MST) marks the midpoint of the zero-velocity phase following the IC. The search region extends from the IC to either the next MSW peak or the maximum stride time limit. To qualify, the region must contain a contiguous segment where all samples fall within the zero-velocity margin (arrow i in Figure 4) and whose duration meets a minimum length requirement (arrow h). The midpoint of this segment is the MST.

Stride Border Definition

A valid stride requires the successful detection of all four gait events: TC, MSW, IC, and MST. If any of the specified conditions are not met, the stride candidate and related events are discarded. In this study, the TC defines the start of a stride, while the subsequent TC marks its conclusion.

2.3.3 Estimation of Temporal Gait Parameters

Based on detected gait events, the system computes the following temporal gait parameters: stride time defined as the time interval between two consecutive TC events, swing time defined as the interval between a TC and the subsequent IC, and stance time, which is the interval between an IC and the next TC.

In addition, the swing and stance phases are expressed as percentages of the stride time, representing the relative durations of the swing and stance periods within each stride.

2.4 Labeling

2.4.1 Motion Detection

For both FallRiskPD and TestES datasets, we applied an offline morphological filtering approach to the norm of the gyroscope signal to identify motion segments that occurred during activities of daily living, as well as lab recordings. First, we applied a 6 Hz low-pass filter to suppress high-frequency artifacts. We then extracted the upper and lower signal envelopes using morphological closing and opening operations, respectively, and computed their mean, to which a threshold was applied to distinguish motion from non-motion periods. Finally, we removed short-duration or low-amplitude segments and merged adjacent motion windows during post-processing. The resulting motion labels were manually reviewed and corrected. In addition, gait segments within these motion periods were then identified based on the labeled stride segmentation described below (section 2.4.2).

2.4.2 Gait Analysis

Stride Segmentation

We used manual annotation produced by Roth et al. [12] for the FallRiskPD due to the irregular and heterogeneous gait patterns characteristic of PD, for which automated segmentation methods are less robust. Dynamic Time Warping (DTW) was used for TestES, both because it represents the state-of-the-art offline method typically applied in practice, where manual labeling is rarely performed, and because it has been shown to achieve high accuracy on gait recorded under supervised conditions [32, 35–37].

Gait Events and Parameters

For both datasets, gait events, including IC, TC, and MST, as well as the temporal gait parameters, including stride time, swing time, and stance time, were identified using a state-of-the-art offline algorithm [38, 39].

2.5 Parameter Optimization

2.5.1 Motion Detection

The motion detection parameters were optimized for each IMU signal's modality (individual Acc and Gyr axes as well as their respective norms) over two coupled components: (i) the decision threshold, and (ii) the validation window size. A random search with 15 parameter combinations was performed for each signal modality, resulting in a total search space of 120 configurations. Parameter values were sampled from predefined, empirically determined ranges to cover a broad set of plausible detector configurations (Table 2). Parameter selection was performed through 4-fold cross-validation (CV) on the FallRiskPD home recordings, as they contain activities of daily living and thus provide a more sensitive and less biased basis for tuning. In each fold, candidate parameters were fitted on the training split and evaluated on the corresponding validation split. Performance was assessed using the F1-score of total motion segments and gait recall, to specifically ensure that true walking periods were not missed.

2.5.2 Gait Analysis

The gait event detection algorithm includes nine tunable parameters as introduced in subsubsection 2.3.2. These were optimized using a random search combined with 4-fold CV on the FallRiskPD dataset.

In the first stage, 100 parameter combinations were randomly sampled from empirically defined ranges (Table 2) and evaluated via cross-validation on the FallRiskPD laboratory recordings, which include slow, preferred, and fast walking conditions. These recordings capture the lower and upper bounds of patients' walking capacity, representing a broad and potentially more extreme range of walking patterns than typically observed in daily life, thereby reducing the search space efficiently. Parameter sets meeting a minimum F1-score threshold of 80% were retained, yielding 37 candidate configurations (37% of the initial sample). In the second stage, these 37 configurations were further evaluated on the FallRiskPD home recordings using 4-fold CV, refining the search to fit the characteristics of unconstrained activities of daily living.

Both in motion detection and gait analysis, all folds were defined at the participant level; no recordings or strides from a participant appeared in more than one fold. The final configuration was selected based on consistency across folds. The parameter combination achieving the best performance in the greatest number of folds was chosen, favoring stability over marginal performance gains in any single fold. Eventually, we tested the final parameter set without further tuning on the independent TestES dataset.

2.6 Evaluation

2.6.1 Motion Detection

For motion detection, performance was evaluated against the reference method using sample-based metrics, including F1-score, recall, precision, and specificity. In addition,

Table 2: Parameter ranges for random search and chosen values from cross-validation for the motion detection and gait analysis algorithm. For motion detection, threshold ranges and chosen values are shown for each IMU signal: Gyr and Acc axes (reported as x / y / z), and their respective norms. The box shows the best performer of the IMU Signal & Threshold parameter combination. The validation window size is reported only for the selected Gyr norm signal.

Parameter		Lower Limit	Upper Limit	Chosen Value
Motion Detection				
IMU Signal & Threshold	Gyr x/y/z [°/s]	5	50	24 / 24 / 24
	Gyr norm [°/s]	10	70	**38**
	Acc x/y/z [m/s^2]	5	15	10 / 10 / 11
	Acc norm [m/s^2]	10	20	20
Validation Window [s]		0.5	5	2.622
Gait Analysis				
Min. Stride Time [s]		0.3	0.9	0.576
Max. Stride Time [s]		1.5	4.0	2.320
Min. MSW Threshold [°/s]		-150	-80	-95.032
Max. MSW Threshold [°/s]		-180	-110	-141.226
Max. TC to MSW distance [s]		0.2	0.6	0.459
Max. MSW to IC distance [s]		0.3	0.8	0.684
Min. IC amplitude [°/s]		0	80	57.357
Min. Zero Velocity Duration [s]		0.05	0.40	0.167
Zero Velocity Amplitude Margin [°/s]		10	40	39.642

gait recall was computed to quantify the proportion of gait that was captured within the detected motion segments. This metric assesses how effectively the motion detector preserves true walking periods without missing gait. Furthermore, the best-performing configuration in the FallRiskPD-home dataset is reported. Results are reported as mean ± standard deviation across participants, with each participant representing a single independent data point.

2.6.2 Gait Analysis

We evaluated the system's performance on two levels: stride segmentation and gait event timing errors. The former complements the latter by quantifying stride detection performance, since small event timing errors do not necessarily imply good overall system performance when only a limited subset of strides is detected.

Stride Detection

Performance is evaluated using the F1-score, recall, precision, and specificity. A stride is classified as a true positive (TP) if both stride borders (start and end) fall within ±100 m s of the reference stride borders. one-to-one stride-matching rule used to prevent multiple detections matching the same reference stride. Results are reported as

mean ± standard deviation across participants, with each participant representing a single independent data point.

As described in section 2.4.2, the proposed real-time method is evaluated against the hand-labeled ground truth in the FallRiskPD, and it is evaluated against DTW as the offline reference method in the TestES [12, 35, 37, 39, 40].

Gait Events and Parameters

For each matched stride, signed error (Equation 1) and absolute error (Equation 2) are computed for both gait events and gait parameters. The maximal absolute error (Equation 4) is reported only for gait events, as it quantifies the temporal deviation between corresponding event time points. The absolute percentage error (Equation 3) is reported for gait parameters, where it is computed based on duration-related measures, allowing for a meaningful relative comparison.

$$SE = x_{RT} - x_{Reference} \tag{1}$$

$$AE = |x_{RT} - x_{Reference}| \tag{2}$$

$$APE = \frac{|x_{RT} - x_{Reference}|}{x_{Reference}} \times 100\,\% \tag{3}$$

$$\max(AE) = \max(|x_{RT} - x_{Reference}|) \tag{4}$$

Where x_{RT} represents the calculated values detected by the real-time system and $x_{Reference}$ represents the reference method.

Additionally, these metrics are analyzed separately for each walking speed (slow, normal, fast, and free walking) in the TestES dataset. Errors are reported as mean ± standard deviation across all strides of all participants.

2.6.3 Computational Time and Delay

To evaluate computational performance, the runtime of the algorithms executing on the ANNA-B4 evaluation board was measured. Runtime was assessed separately for the motion detection and gait analysis modules, as well as for the complete processing pipeline — including sensor data acquisition, motion detection, gait analysis, and result logging. Execution time was recorded for each incoming data sample, and the mean, standard deviation, and worst-case execution time were computed across all samples.

The algorithm's delay is defined as the cumulative time from the occurrence of a physical gait event to the delivery of the processed result. This delay is influenced by several factors, including filter size, window size, and the runtime required to analyze the data. The delay caused by the analysis window is determined by the time difference between the end of a stride and the end of the analysis window. Eventually, the total delay is calculated by summing the filter size, analysis window delay, and the worst-case execution time.

Table 3: Motion detection results based on Gyr-norm. Gait recall refers to the samples within the reference stride labels correctly classified as motion. The performance metric values are given as mean ± standard deviation across patients.

Dataset	Motion				Gait
	F1-Score [%]	Recall [%]	Precision [%]	Specificity [%]	Recall [%]
FallRiskPD-Home	88.36 ± 4.31	90.99 ± 3.10	86.02 ± 6.16	93.77 ± 3.78	99.95 ± 0.13
TestES	97.96 ± 1.07	99.19 ± 1.21	96.78 ± 1.62	83.41 ± 7.67	99.59 ± 0.09

3 Results

3.1 Motion Detection

The cross-validation procedure converged consistently across all four folds, resulting in a stable optimal configuration using the Gyr-norm as input signal (Table 2). Among Acc-based signals, the norm achieved the best performance with an F1-score of 81.3 % and gait recall of 99.6 %. Nonetheless, the Gyr-norm had the highest performance on the FallRiskPD with an F1-score of 88.4 % across all motion (gait and non-gait) and a gait recall of 99.9 %, demonstrating that nearly all samples within gait segments were correctly detected as motion. Using the optimal parameters on TestES, the real-time system achieved an F1-score of 98.0 % and a gait recall of 99.9 %.

Furthermore, the sample-based relative proportions of non-motion, gait, and non-gait motion show that, during activities of daily living, as captured in the FallRiskPD-Home recordings, non-motion segments accounted for 70 ± 14.8% of total recording time, exceeding gait and non-gait motion segments. By contrast, in the TestES dataset, gait was the dominant class, comprising 72 % of recording time (Figure 5).

3.2 Gait Analysis

The gait analysis parameters also converged consistently across all folds of the cross-validation procedure, resulting in a single optimal parameter set (Table 2). This parameter set was subsequently used for evaluation of the system on the TestES dataset.

3.2.1 Stride Segmentation

The real-time system achieved a higher F1-score on the laboratory recordings compared to the home recordings of patients with PD, with mean values of 93.26% and 85.37%, respectively. On the TestES dataset, the system achieved an F1-score of 95.42%, demonstrating strong agreement with the DTW as the state-of-the-art offline model (Table 4). FallRiskPD results summarize held-out validation folds from participant-level cross-validation, whereas TestES results were obtained on the independent cohort using the fixed parameter set. Participant-level performance metrics treat each participant as one aggregation unit.

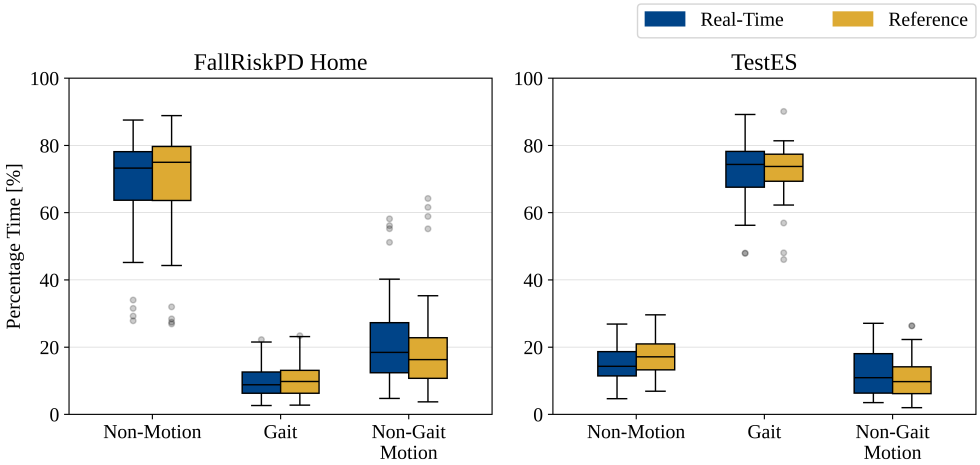


Fig. 5: Relative amount of time of non-motion, gait, and non-gait motions in the home recordings of the FallRiskPD dataset and the TestES dataset. Comparison between the real-time method, the reference labels.

Table 4: Stride segmentation performance of the real-time algorithm compared to the reference labels on the FallRiskPD Lab and Home, and the TestES datasets. The performance metric values are given as mean ± standard deviation across patients.

Dataset	Labeled Strides	Detected Strides	F1-Score [%]	Recall [%]	Precision [%]
FallRiskPD-Lab	19789	17748	93.26 ± 3.77	91.26 ± 5.90	95.63 ± 3.14
FallRiskPD-Home	157862	129973	85.37 ± 7.35	83.43 ± 8.75	88.32 ± 9.09
TestES	7813	7663	95.42 ± 3.71	97.46 ± 4.42	93.71 ± 5.24

3.2.2 Event Detection

Among the three gait events, TC consistently exhibited the lowest absolute error, while MST showed the highest AE across all three datasets. Comparing the datasets, absolute errors were similar, but home recordings showed the highest maximum absolute errors: 0.79 s for TC, 1.31 s for IC, and 3.05 s for MST. Although the absolute errors for IC and MST were higher than the corresponding signed errors, the signed errors remained close to zero, suggesting that timing errors occurred in both directions and did not exhibit systematic bias (Stride Events section in Table 5).

Table 5: Errors of gait event detection and temporal gait parameters for all datasets. Signed error (SE) and absolute error (AE) are given in seconds. The last column reports the maximal absolute error ($max(AE)$) in seconds for the gait events and the absolute percentage error (APE) in percent for the gait parameters.

Category	Events	Dataset	SE [s]	AE [s]	$max(AE)$
Stride Events	TC	FallRiskPD-Lab	0.000 ± 0.009	0.001 ± 0.009	$0.531\,s$
		FallRiskPD-Home	0.001 ± 0.015	0.002 ± 0.015	$0.791\,s$
		TestES	0.000 ± 0.003	0.000 ± 0.003	$0.130\,s$
	IC	FallRiskPD-Lab	0.001 ± 0.029	0.021 ± 0.021	$0.586\,s$
		FallRiskPD-Home	-0.006 ± 0.035	0.024 ± 0.026	$1.311\,s$
		TestES	0.004 ± 0.029	0.021 ± 0.020	$0.490\,s$
	MST	FallRiskPD-Lab	0.000 ± 0.095	0.057 ± 0.077	$1.662\,s$
		FallRiskPD-Home	-0.003 ± 0.124	0.069 ± 0.103	$3.053\,s$
		TestES	0.017 ± 0.096	0.070 ± 0.068	$1.460\,s$
Category	Parameters	Dataset	SE [s]	AE [s]	APE
Gait Parameters	Stride Time	FallRiskPD-Lab	0.002 ± 0.045	0.002 ± 0.045	$0.2 \pm 4.5\,\%$
		FallRiskPD-Home	0.001 ± 0.043	0.003 ± 0.043	$0.3 \pm 4.3\,\%$
		TestES	0.000 ± 0.004	0.000 ± 0.004	$0.0 \pm 0.3\,\%$
	Swing Time	FallRiskPD-Lab	0.000 ± 0.030	0.022 ± 0.021	$5.2 \pm 5.4\,\%$
		FallRiskPD-Home	-0.008 ± 0.034	0.026 ± 0.024	$6.5 \pm 17.2\,\%$
		TestES	0.003 ± 0.026	0.021 ± 0.016	$4.6 \pm 3.4\,\%$
	Stance Time	FallRiskPD-Lab	0.002 ± 0.052	0.023 ± 0.046	$3.2 \pm 7.0\,\%$
		FallRiskPD-Home	0.009 ± 0.052	0.027 ± 0.046	$3.6 \pm 6.9\,\%$
		TestES	-0.003 ± 0.026	0.021 ± 0.016	$2.5 \pm 2.0\,\%$

3.2.3 Temporal Parameters

Among the stride parameters, stride time proved to be the most robust, with an absolute percentage error of only 0.3 % in the home recordings of the FallRiskPD dataset. Swing time and stance time showed moderately higher errors of 6.5 % and 3.6 %, respectively, in the same recordings.

In the TestES dataset, the absolute percentage error was lower compared to the home recordings, with 4.6 % for the swing time and 2.5 % for the stance time. Although the absolute error of stance time was comparable to that of swing time (0.021 s), its signed error was negatively shifted, indicating more incidents occurring after the offline reference method (Gait parameter section in Table 5).

Figure 6 presents pooled stride-level agreement between the real-time system and the offline DTW reference in TestES dataset for all temporal gait parameters using Bland-Altman plots. The influence of walking speed is illustrated by differences at the stride level according to the walking speed. The error for the stride time is zero-centered, with margins falling below ±0.01 s across all speeds. A distinct alignment of samples at zero difference is visible across the full range of stride times, with only minor outliers present during free and fast walking. For swing and stance time as

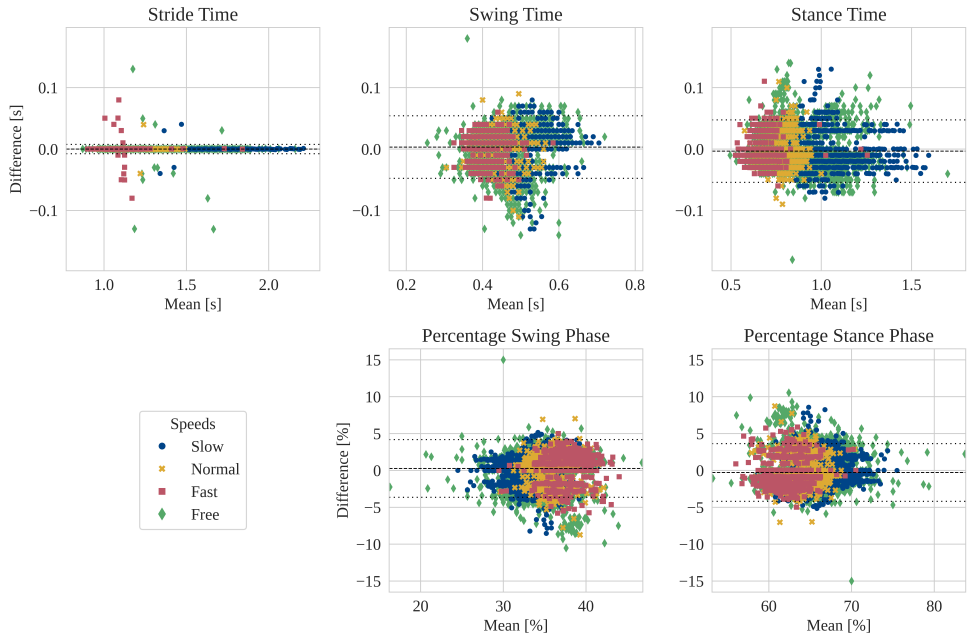


Fig. 6: Bland–Altman plots of temporal gait parameters for the TestES dataset, stratified by walking speed. The plots display Stride, Swing, and Stance Time (in seconds) alongside Percentage Swing and Stance Phase (in %). Markers represent specific speed conditions: Slow (blue circles), Normal (orange crosses), Fast (red squares), and Free (green diamonds). The central dashed line indicates the overall mean difference (bias), while the dotted lines represent the 95% limits of agreement.

well as for the percentage swing and stance phases, the errors are zero-centered too. However, compared to the stride time, they all show a higher deviation, with error margins below 0.05 s for the swing and stance time and 4.5 % for the percentage swing and stance phase.

3.3 Computational Time and Delay

The motion detection algorithm required an average runtime of 0.025 ms, with a worst-case execution time of 0.201 ms. The gait analysis runtime scaled with the analysis window size; for the selected 3 s window, the worst-case runtime was 5.865 ms.

The total system runtime, including sensor data retrieval and Bluetooth logging, had an average runtime of 1.245 ms per data sample. The worst-case execution time for the complete system was 9.219 ms. The average processing delay for delivering the parameters of a stride comprises 1.169 ± 0.525 s for a gait analysis window of three seconds.

Table 6: Computational time measure for the two main algorithm parts, motion detection and gait analysis, as well as for the total system including reading sensor signal data, processing the signal, and logging the signal.

	Average [ms]	Worst-Case [ms]
Motion Detection	0.025 ± 0.012	0.201
Gait Analysis	0.032 ± 0.345	5.865
Total	1.245 ± 0.578	9.219

4 Discussion

This study presents a portable, lightweight, compact, real-time gait analysis system implemented on an embedded platform for continuous on-device monitoring. The proposed method comprises two sequential components of motion detection followed by gait analysis. Validation using home recordings from individuals with PD, together with real-time testing on the embedded platform, demonstrates that the proposed system achieves low error and enables reliable, continuous gait monitoring in practical patient-care settings.

The proposed system adopts a two-stage pipeline in which motion detection precedes gait analysis such that gait parameters are computed only when relevant movement is present. This two-stage pipeline represents a key contribution for real-world home monitoring, where large portions of wearable data do not correspond to walking. This is supported by the observation that $70 \pm 14.8\%$ of home-recorded data consisted of non-motion segments, which can be safely excluded from downstream processing (Figure 5). By skipping the gait analysis stage during non-motion segments, the proposed framework is able to reduce computational load and processing latency. Additional power-saving strategies, such as adaptive sampling rates or sleep modes, may further enhance efficiency but were beyond the scope of the present study and warrant future investigation.

The motion detection module achieved its best performance using the Gyr-norm signal, with a gait recall of 99.9%. Furthermore, among the accelerometer-based signals, the Acc-norm performed best, achieving a gait recall of 99.6%. Given that accelerometer sampling is reported to consume less power than Gyr sampling [41], this performance–energy trade-off suggests that Acc-norm may be preferable for motion detection in practice: the Gyr can be fully powered down during non-motion segments, could reduce energy use, subject to direct power and battery-life measurements at a modest cost to recall.

Across all metrics, i.e., the number of detected strides and the error of detected events, performance was highest in healthy control participants (TestES), followed by laboratory recordings of patients with PD (FallRiskPD), and lowest in home recordings of patients with PD. This performance gradient stems from increased gait impairment

and movement variability, as well as potential sensor misalignment and environmental artifacts in real-world home monitoring. These findings are consistent with prior work using different algorithms, which has shown systematic gait differences between healthy controls and patients with PD [36], as well as laboratory and free-living gait [11, 12, 42, 43]. Compared to state-of-the-art offline methods evaluated on the same dataset and labels, our model achieved F1-scores of 93.2% and 85.3% (PD lab and home), closely matching the DTW-based method (94.6% and 85.1%) and remaining competitive with the more computationally intensive HMM-based method (96.2% and 92.4%). This indicates that our real-time model performs comparably to offline approaches, including those requiring substantially greater computational resources. Additionally, when taking DTW as the reference point, our model further achieved an F1-score of 95.4% on the TestES dataset, reinforcing this finding.

Regarding gait events and temporal parameter estimation, differences across specific events were largely attributable to methodological similarities or differences with the reference pipeline [38]. For example, TC is computed similarly in both approaches based on zero-crossings of the Gyr signal, whereas MST in the reference method [38] relies on multi-axis energy minimization, in contrast to the axis-specific constraints required for real-time implementation in the proposed system. Overall, the proposed real-time system achieved low average errors in gait event detection and temporal parameter estimation, with laboratory performance comparable to previously reported real-time approaches, including both rule-based methods [26, 27, 29, 43, 44] and data-driven approaches [21, 23, 24, 31]. These results indicate that a carefully designed two-stage, heuristic pipeline can provide reliable real-time gait analysis in both controlled and real-world home settings, offering an efficient and practical alternative to more computationally demanding ML-based approaches for continuous patient monitoring.

From a computational perspective, real-time gait analysis on wearable embedded systems is fundamentally constrained by the interplay between algorithmic complexity, energy consumption, and hardware size, which collectively determine portability and practical usability. Increasing model complexity typically necessitates more capable hardware [21, 23, 24, 31], larger form factors [20, 22], or multi-sensor configurations [18, 22], thus limiting practical usability for continuous home monitoring. While methodological advances in machine-learning and deep-learning approaches continue to push the field forward, this work deliberately prioritizes practicality for end users-patients with movement disorders-by focusing on a lightweight, compact design that can be comfortably worn during daily-life activities. Accordingly, the proposed hardware footprint of approximately 2.5 x 3.5 cm is substantially smaller than comparable embedded gait analysis systems, such as the design reported by Wu et al. [20] (6.1 x 4.7 cm) or Lu et al. [22] using a Raspberry Pi-4B (8.5 x 5.6 cm). In addition, the proposed pipeline achieves a lower end-to-end run-time of 1.2 ms per processing cycle in healthy participants under live conditions, compared to 20 ms reported by Wu et al. [20] and 39 ms by Lu et al. [22]. Notably, since the underlying pipeline and algorithm for parameter estimation do not differ between populations. The same pipeline achieved reliable performance on real-world activities of daily living in patients with

PD, providing evidence about algorithm behavior on PD signals. However, equivalent live performance in people with PD cannot be inferred and remains to be tested.

The clinical relevance of the proposed system lies in its design for continuous, real-world monitoring of daily mobility in people with PD. In contrast to most existing real-time gait analysis systems, which are primarily evaluated on healthy participants or under controlled, task-oriented laboratory protocols, the present work provides a comprehensive evaluation on extended home recordings from PD patients, capturing the variability and artifacts inherent to daily-life walking. To the best of our knowledge, this represents one of the first studies to systematically investigate real-time gait analysis under such unconstrained home monitoring conditions in this population.

Motor fluctuations in PD, driven by factors such as wearing-off phenomena, will manifest themselves as changes in gait parameters, including temporal gait parameters throughout the day [4, 42]. Capturing these variations is clinically relevant, as they play an important role for patients, caregivers, and clinicians in disease management and in improving quality of life [7, 45]. Additionally, the observed errors in temporal gait parameters fall within the range of variability reported for clinically relevant gait alterations, including changes preceding freezing of gait or fall-related episodes [46–50]. The low-latency, real-time processing strategy of the proposed system offers a strong foundation for future studies targeting freezing-of-gait and fall-related events directly, enabling continuous monitoring of gait dynamics with minimal delay and opening a path toward longitudinal progression monitoring.

Overall, the ability to capture gait under unconstrained home conditions in people with PD represents an important step toward ecologically valid mobility assessment, where motor fluctuations and medication-related changes are reflected in temporal gait variability throughout the day. Our findings indicate that the proposed lightweight system represents a step toward real-world deployment, offering a practical and scalable approach for continuous patient-centered gait monitoring and providing a foundation for future extensions toward clinical decision support and symptom tracking.

4.1 Limitations

Several limitations should be considered when interpreting the results of this study.

First, the annotation of motion segments in home recordings is subject to inherent uncertainty, as they were defined based on the signal rather than explicit knowledge of the performed activities. Additionally, motion reference labels were initially derived from Gyr-y signals and subsequently reviewed manually; this may have favored gyroscope-based detectors relative to accelerometer-based alternatives.

Second, stride annotations in the home environment were restricted to walking bouts of more than four consecutive strides, which may have resulted in the exclusion of strides in shorter walking bouts.

Third, live real-time testing on the unseen TestES dataset was limited to healthy participants walking in a supervised environment, as deploying the sensor hardware for unsupervised real-world use in patients with PD was outside the ethical and logistical scope of the current validation stage. Since hyperparameter selection and performance estimation on the PD cohort used the same cross-validation framework, FallRiskPD results constitute internal validation and may be optimistic. Therefore, testing the final

product on patients with PD during unsupervised activities of daily living remains necessary.

5 Conclusions

The present work introduces a lightweight, real-time gait analysis system implemented on an embedded ANNA B4 chip for continuous monitoring of daily-life mobility in patients with PD. The system was evaluated in patients with PD under both laboratory and home conditions and tested on healthy control participants, enabling assessment across increasingly unconstrained and ecologically valid scenarios. Across these settings, the proposed approach maintained low computational latency and competitive accuracy in temporal gait parameters, despite the increased variability inherent to real-world recordings. The achieved temporal resolution and real-time processing indicate that the system can capture gait dynamics at a scale relevant to clinically meaningful alterations reported in association with freezing of gait and fall-related events, without implying direct event detection. Together, these findings demonstrate that the combination of a lightweight motion-detection stage and an efficient gait analysis pipeline enables continuous, low-power wearable operation, offering a promising basis for future real-world home deployment. By targeting long-term, unobtrusive monitoring of daily mobility, the proposed system provides a practical foundation for patient-centered gait assessment that may assist patients, caregivers, and clinicians in tracking mobility changes and treatment-related effects. While this work focuses on system design and validation, the demonstrated real-time capability establishes a basis for future studies targeting feedback-based interventions and the investigation of clinically relevant gait events, subject to dedicated clinical validation.

Acknowledgements. The authors gratefully acknowledge Portabiles HealthCare Technologies GmbH for leading and coordinating the NoFreeze project. We sincerely thank all study participants and everyone who contributed to the planning and conduct of the study, particularly those who supported participant recruitment, data collection, and study organization.

Declarations

Medtech Ingenieur GmbH designed the sensors used in the study but did not control the study design, data analysis, interpretation of the results, or decision to submit the manuscript for publication.

Funding

This research was partially funded by the German Federal Ministry of Education and Research (BMBF) as part of the research program “Interactive technologies for health and quality of life.”

Data collection for this study was supported by the Bavarian Ministry for Economy, Regional Development and Energy through the Medical Valley Award 2017 (FallRiskPD project).

Competing of interests

At the time the study was conducted, Jelina Unger was a student at Friedrich-Alexander-Universität Erlangen-Nürnberg (FAU) and was employed as a working student by Medtech Ingenieur GmbH. Goran Madzar is the managing director at Medtech Ingenieur GmbH. Medtech Ingenieur GmbH manufactured the sensor system used in this study.

Ethics approval and consent to participate

The study was approved by the local ethics committee of the Friedrich-Alexander-University Erlangen-Nuremberg, Germany (approval numbers 165_18B and 106_13B). All participants provided written informed consent before data collection.

Consent for publication

Not applicable

Availability of data and materials

The datasets used and/or analyzed during the current study are available from the corresponding author on reasonable request and after approval by the ethical committee in case patient-related data is requested.

Author contribution

JU performed the implementation and evaluation of the methods, analyzed the data, and drafted the manuscript. GM contributed to the development of the sensors and embedded hardware system. AKS contributed to the study design. FM, HG, and JW supported the data acquisition. SS, IG, and MD contributed to the preparation and revision of the manuscript. BE, HG, and JW supervised the overall conception and design of the work. HM conceived and supervised the study, contributed to the methodology and interpretation of the results, and led the revision of the manuscript. All authors read and approved the final manuscript.

List of Abbreviations

Acc Accelerometer
CV cross-validation
DTW Dynamic Time Warping
Gyr Gyroscope
IC initial contact
IMU Inertial Measurement Unit
MST mid-stance
MSW mid-swing
PD Parkinson's Disease
TC terminal contact
TP true positive

References

[1] Pau, M., Mulas, I., Putzu, V., Asoni, G., Viale, D., Mameli, I., Leban, B., Allali, G.: Smoothness of Gait in Healthy and Cognitively Impaired Individuals: A Study on Italian Elderly Using Wearable Inertial Sensor. Sensors **20**(12), 3577 (2020) https://doi.org/10.3390/s20123577

[2] Hardy, S.E., Perera, S., Roumani, Y.F., Chandler, J.M., Studenski, S.A.: Improvement in Usual Gait Speed Predicts Better Survival in Older Adults. Journal of the American Geriatrics Society **55**(11), 1727–1734 (2007) https://doi.org/10.1111/j.1532-5415.2007.01413.x

[3] Mirelman, A., Bonato, P., Camicioli, R., Ellis, T.D., Giladi, N., Hamilton, J.L., Hass, C.J., Hausdorff, J.M., Pelosin, E., Almeida, Q.J.: Gait impairments in Parkinson's disease. The Lancet Neurology **18**(7), 697–708 (2019) https://doi.org/10.1016/S1474-4422(19)30044-4

[4] Moradi, H., Roth, N., Seifer, A.-K., Eskofier, B.M.: Detection of distorted gait and wearing-off phenomenon in Parkinson's disease patients during Levodopa therapy. In: 2022 IEEE-EMBS International Conference on Biomedical and Health Informatics (BHI), pp. 01–04. IEEE, Ioannina, Greece (2022). https://doi.org/10.1109/BHI56158.2022.9926873

[5] Atrsaei, A., Corrà, M.F., Dadashi, F., Vila-Chã, N., Maia, L., Mariani, B., Maetzler, W., Aminian, K.: Gait speed in clinical and daily living assessments in Parkinson's disease patients: Performance versus capacity. npj Parkinson's Disease **7**(1), 24 (2021) https://doi.org/10.1038/s41531-021-00171-0

[6] Mao, Y., Ogata, T., Ora, H., Tanaka, N., Miyake, Y.: Estimation of stride-by-stride spatial gait parameters using inertial measurement unit attached to the shank with inverted pendulum model. Scientific Reports **11**(1), 1391 (2021) https://doi.org/10.1038/s41598-021-81009-w

[7] Marxreiter, F., Gaßner, H., Borozdina, O., Barth, J., Kohl, Z., Schlachetzki, J.C.M., Thun-Hohenstein, C., Volc, D., Eskofier, B.M., Winkler, J., Klucken, J.: Sensor-based gait analysis of individualized improvement during apomorphine titration in Parkinson's disease. Journal of Neurology **265**(11), 2656–2665 (2018) https://doi.org/10.1007/s00415-018-9012-7

[8] Schlachetzki, J.C.M., Barth, J., Marxreiter, F., Gossler, J., Kohl, Z., Reinfelder, S., Gassner, H., Aminian, K., Eskofier, B.M., Winkler, J., Klucken, J.: Wearable sensors objectively measure gait parameters in Parkinson's disease. PLOS ONE **12**(10), 0183989 (2017) https://doi.org/10.1371/journal.pone.0183989

[9] Gao, S., Chen, J., Dai, Y., Hu, B.: Wearable Systems Based Gait Monitoring and Analysis. Springer, Cham, Switzerland (2022)

[10] Prasanth, H., Caban, M., Keller, U., Courtine, G., Ijspeert, A., Vallery, H., Von Zitzewitz, J.: Wearable Sensor-Based Real-Time Gait Detection: A Systematic Review. Sensors (Basel, Switzerland) **21**(8) (2021)

[11] Sidoroff, V., Moradi, H., Prigent, G., Jagusch, F., Teckenburg, I., Asalian, M., Hergenroeder-Lenzner, N., Giraitis, M., Schoenfeldt-Reichmann, E.T., Ndayisaba, J.-P., Goebel, G., Seppi, K., Ionescu, A., Krismer, F., Benninger, D., Winkler, J., Eskofier, B.M., Klucken, J., Aminian, K., Wenning, G., Sapienza, S., Gassner, H., Raccagni, C., MobilityAPP Study Group: Moving beyond the hospital: In-depth characterization of daily-life mobility in patients with atypical Parkinsonian disorders. npj Parkinson's Disease **12**(1), 34 (2026) https://doi.org/10.1038/s41531-025-01242-2

[12] Roth, N., Küderle, A., Ullrich, M., Gladow, T., Marxreiter, F., Klucken, J., Eskofier, B.M., Kluge, F.: Hidden Markov Model based stride segmentation on unsupervised free-living gait data in Parkinson's disease patients. Journal of NeuroEngineering and Rehabilitation **18**(1), 93 (2021) https://doi.org/10.1186/s12984-021-00883-7

[13] Hutabarat, Y., Owaki, D., Hayashibe, M.: Recent Advances in Quantitative Gait Analysis Using Wearable Sensors: A Review. IEEE Sensors Journal **21**(23), 26470–26487 (2021)

[14] Jourdan, T., Debs, N., Frindel, C.: The Contribution of Machine Learning in the Validation of Commercial Wearable Sensors for Gait Monitoring in Patients: A Systematic Review. Sensors **21**(14), 4808 (2021) https://doi.org/10.3390/s21144808

[15] Romijnders, R., Warmerdam, E., Hansen, C., Schmidt, G., Maetzler, W.: A Deep Learning Approach for Gait Event Detection from a Single Shank-Worn IMU: Validation in Healthy and Neurological Cohorts. Sensors **22**(10), 3859 (2022) https://doi.org/10.3390/s22103859

[16] Dumphart, B., Slijepcevic, D., Zeppelzauer, M., Kranzl, A., Unglaube, F., Baca, A., Horsak, B.: Robust deep learning-based gait event detection across various pathologies. PLOS ONE **18**(8), 0288555 (2023) https://doi.org/10.1371/journal.pone.0288555

[17] Larsen, A.G., Sadolin, L.Ø., Thomsen, T.R., Oliveira, A.S.: Accurate detection of gait events using neural networks and IMU data mimicking real-world smartphone usage. Computer Methods in Biomechanics and Biomedical Engineering, 1–11 (2024) https://doi.org/10.1080/10255842.2024.2423252

[18] Karakish, M., Fouz, M.A., ELsawaf, A.: Gait Trajectory Prediction on an Embedded Microcontroller Using Deep Learning. Sensors **22**(21), 8441 (2022) https://doi.org/10.3390/s22218441

[19] Shayne, M., Molina, L.A., Hu, B., Chomiak, T.: Implementing Gait Kinematic Trajectory Forecasting Models on an Embedded System. Sensors **24**(8), 2649 (2024) https://doi.org/10.3390/s24082649

[20] Wu, J., Becsek, B., Schaer, A., Maurenbrecher, H., Chatzipirpiridis, G., Ergeneman, O., Pané, S., Torun, H., Nelson, B.J.: Real-Time Gait Phase Detection on Wearable Devices for Real-World Free-Living Gait. IEEE Journal of Biomedical and Health Informatics **27**(3), 1295–1306 (2023) https://doi.org/10.1109/JBHI.2022.3228329

[21] Wang, F.-C., Li, Y.-C., Kuo, T.-Y., Chen, S.-F., Lin, C.-H.: Real-Time Detection of Gait Events by Recurrent Neural Networks. IEEE Access **9**, 134849–134857 (2021) https://doi.org/10.1109/ACCESS.2021.3116047

[22] Lu, Y., Zhu, J., Chen, W., Ma, X.: An IMU-Based Real-Time Gait Detection Method for Intelligent Control of Knee Assistive Devices. IEEE Transactions on Instrumentation and Measurement **72**, 1–9 (2023) https://doi.org/10.1109/TIM.2023.3329222

[23] Vajs, I.A., Bobic, V.N., Duric-Jovicic, M.D., Jankovic, M.M.: Open-source application for real-time gait analysis using inertial sensors. In: 2020 28th Telecommunications Forum (TELFOR), pp. 1–4. IEEE, Belgrade, Serbia (2020). https://doi.org/10.1109/TELFOR51502.2020.9306636

[24] Kidziński, Ł., Delp, S., Schwartz, M.: Automatic real-time gait event detection in children using deep neural networks. PLOS ONE **14**(1), 0211466 (2019) https://doi.org/10.1371/journal.pone.0211466

[25] González, R.C., López, A.M., Rodriguez-Uría, J., Álvarez, D., Alvarez, J.C.: Real-time gait event detection for normal subjects from lower trunk accelerations. Gait & Posture **31**(3), 322–325 (2010) https://doi.org/10.1016/j.gaitpost.2009.11.014

[26] Allseits, E., Lučarević, J., Gailey, R., Agrawal, V., Gaunaurd, I., Bennett, C.: The development and concurrent validity of a real-time algorithm for temporal gait analysis using inertial measurement units. Journal of Biomechanics **55**, 27–33 (2017) https://doi.org/10.1016/j.jbiomech.2017.02.016

[27] Maqbool, H.F., Husman, M.A.B., Awad, M.I., Abouhossein, A., Iqbal, N., Dehghani-Sanij, A.A.: A Real-Time Gait Event Detection for Lower Limb Prosthesis Control and Evaluation. IEEE transactions on neural systems and rehabilitation engineering : a publication of the IEEE Engineering in Medicine and Biology Society **25**(9), 1500–1509 (2017)

[28] Akhetova, S.M., Roembke, R., Adamczyk, P.: Detecting Toe-Off and Initial Contact in Real-Time With Self-Adapting Thresholds. Journal of Biomechanical Engineering **146**(11), 114502 (2024) https://doi.org/10.1115/1.4065842

[29] Liu, Y., Liu, X., Zhu, Q., Chen, Y., Yang, Y., Xie, H., Wang, Y., Wang, X.: Adaptive Detection in Real-Time Gait Analysis through the Dynamic Gait Event Identifier. Bioengineering **11**(8), 806 (2024) https://doi.org/10.3390/bioengineering11080806

[30] Hua, R., Wang, Y.: Monitoring Insole (MONI): A Low Power Solution Toward Daily Gait Monitoring and Analysis. IEEE Sensors Journal **19**(15), 6410–6420 (2019)

[31] Wu, J., Kuruvithadam, K., Schaer, A., Stoneham, R., Chatzipirpiridis, G., Awai, C.E., Barry, G., Martin, J., Pané, S., Nelson, B., Ergeneman, O., Torun, H.: An intelligent in-shoe system for gait monitoring and analysis with optimized sampling and real-time visualization capabilities. Sensors (Basel, Switzerland) **21** (2021) https://doi.org/10.3390/s21082869

[32] Voisard, C., De l'Escalopier, N., Ricard, D., Oudre, L.: Automatic gait events detection with inertial measurement units: Healthy subjects and moderate to severe impaired patients. Journal of NeuroEngineering and Rehabilitation **21**(1), 104 (2024) https://doi.org/10.1186/s12984-024-01405-x

[33] Ferraris, F., Gorini, I., Grimaldi, U., Parvis, M.: Calibration of three-axial rate gyros without angular velocity standards **42**(1), 446–449 https://doi.org/10.1016/0924-4247(94)80031-6 . Accessed 2026-02-07

[34] Küderle, A., Roth, N., Richer, R., Eskofier, B.M.: imucal - a python library to calibrate 6 DOF IMUs **7**(73), 4338 https://doi.org/10.21105/joss.04338 . Accessed 2026-02-07

[35] Barth, J., Oberndorfer, C., Kugler, P., Schuldhaus, D., Winkler, J., Klucken, J., Eskofier, B.: Subsequence dynamic time warping as a method for robust step segmentation using gyroscope signals of daily life activities. In: 2013 35th Annual International Conference of the IEEE Engineering in Medicine and Biology Society (EMBC), pp. 6744–6747. IEEE, Osaka (2013). https://doi.org/10.1109/EMBC.2013.6611104

[36] Haji Ghassemi, N., Hannink, J., Martindale, C.F., Gaßner, H., Müller, M., Klucken, J., Eskofier, B.M.: Segmentation of Gait Sequences in Sensor-Based Movement Analysis: A Comparison of Methods in Parkinson's Disease. Sensors (Basel, Switzerland) **18**(1) (2018)

[37] Šprager, S., Jurič, M.: Robust Stride Segmentation of Inertial Signals Based on Local Cyclicity Estimation. Sensors **18**(4), 1091 (2018) https://doi.org/10.3390/s18041091

[38] Rampp, A., Barth, J., Schülein, S., Gaßmann, K.-G., Klucken, J., Eskofier, B.M.: Inertial sensor-based stride parameter calculation from gait sequences in geriatric patients. IEEE transactions on bio-medical engineering **62**(4), 1089–1097 (2015)

[39] Küderle, A., Ullrich, M., Roth, N., Ollenschläger, M., Ibrahim, A.A., Moradi, H., Richer, R., Seifer, A.-K., Zürl, M., Sîmpetru, R.C., Herzer, L., Prossel, D., Kluge, F., Eskofier, B.M.: Gaitmap—An Open Ecosystem for IMU-Based Human Gait Analysis and Algorithm Benchmarking. IEEE Open Journal of Engineering in Medicine and Biology **5**, 163–172 (2024) https://doi.org/10.1109/OJEMB.2024.3356791

[40] Steinmetzer, T., *et al.*: Comparison of algorithms and classifiers for stride detection using wearables. Neural Computing and Applications **32**(24), 17857–17868 (2020) https://doi.org/10.1007/s00521-019-04384-6

[41] Liu, Q., Williamson, J., Li, K., Mohrman, W., Lv, Q., Dick, R.P., Shang, L.: Gazelle: Energy-Efficient Wearable Analysis for Running **16**(9), 2531–2544 https://doi.org/10.1109/TMC.2016.2623304 . Accessed 2026-07-20

[42] Del Din, S., Godfrey, A., Mazzà, C., Lord, S., Rochester, L.: Free-Living Monitoring of Parkinson's Disease: Lessons from the Field. Movement disorders : official journal of the Movement Disorder Society **31**(9), 1293–1313 (2016)

[43] Perez-Ibarra, J.C., Siqueira, A.A.G., Krebs, H.I.: Real-Time Identification of Gait Events in Impaired Subjects Using a Single-IMU Foot-Mounted Device. IEEE Sensors Journal **20**(5), 2616–2624 (2020) https://doi.org/10.1109/JSEN.2019.2951923

[44] Gouwanda, D., Gopalai, A.A.: A robust real-time gait event detection using wireless gyroscope and its application on normal and altered gaits. Medical Engineering & Physics **37**(2), 219–225 (2015) https://doi.org/10.1016/j.medengphy.2014.12.004

[45] Moradi, H., Hannink, J., Stallforth, S., Gladow, T., Ringbauer, S., Mayr, M., Winkler, J., Klucken, J., Eskofier, B.M.: Monitoring medication optimization in patients with Parkinson's disease. In: 2023 45th Annual International Conference of the IEEE Engineering in Medicine & Biology Society (EMBC), pp. 1–4. IEEE, Sydney, Australia (2023). https://doi.org/10.1109/EMBC40787.2023.10340618

[46] Ferster, M.L., Mazilu, S., Tröster, G.: Gait Parameters Change Prior to Freezing in Parkinson's Disease: A Data-Driven Study with Wearable Inertial Units. In: Proceedings of the 10th EAI International Conference on Body Area Networks. ICST, Sydney, Australia (2015). https://doi.org/10.4108/eai.28-9-2015.2261411

[47] Silva De Lima, A.L., Evers, L.J.W., Hahn, T., Bataille, L., Hamilton, J.L., Little, M.A., Okuma, Y., Bloem, B.R., Faber, M.J.: Freezing of gait and fall detection in Parkinson's disease using wearable sensors: A systematic review. Journal of Neurology **264**(8), 1642–1654 (2017) https://doi.org/10.1007/s00415-017-8424-0

[48] Borzì, L., Demrozi, F., Bacchin, R.A., Turetta, C., Sigcha, L., Rinaldi, D., Fazzina, G., Balestro, G., Picelli, A., Pravadelli, G., Olmo, G., Tamburin, S., Lopiano,

L., Artusi, C.A.: Freezing of gait detection: The effect of sensor type, position, activities, datasets, and machine learning model. Journal of Parkinson's Disease **15**(1), 163–181 (2025) https://doi.org/10.1177/1877718X241302766

[49] Schniepp, R., Huppert, A., Decker, J., Schenkel, F., Schlick, C., Rasoul, A., Dieterich, M., Brandt, T., Jahn, K., Wuehr, M.: Fall prediction in neurological gait disorders: differential contributions from clinical assessment, gait analysis, and daily-life mobility monitoring. Journal of Neurology **268**, 3421–3434 (2021) https://doi.org/10.1007/s00415-021-10504-x

[50] Ehrhardt, A., Hostettler, P., Widmer, L., Reuter, K., Petersen, J., Straumann, D., Filli, L.: Fall-related functional impairments in patients with neurological gait disorder. Scientific Reports **10** (2020) https://doi.org/10.1038/s41598-020-77973-4

Supplementary Files

This is a list of supplementary files associated with this preprint. Click to download.

- gaitanalysisexample.mp4